Time-Domain Receiver Design for MIMO Underwater Acoustic Communications

Jun Tao[†], Yahong Rosa Zheng[§], Chengshan Xiao[§], T. C. Yang[‡] and Wen-Bin Yang[*]

[†]Dept. of Electrical & Computer Eng., University of Missouri-Columbia, MO 65211, USA

[§]Dept. of Electrical & Computer Eng., Missouri University of Science & Technology, Rolla, MO 65409, USA

[‡]Naval Research Laboratory, Washington, DC 20375, USA

[*]National Institute of Standards and Technology, Gaithersburg, MD 20899, USA

Abstract—**In this paper, we propose a time-domain receiver design scheme for high data rate single carrier multiple-input, multiple-output (MIMO) underwater acoustic communications. In this scheme, each received packet is artificially partitioned into blocks for processing. The MIMO channel is initially estimated using training blocks at the front of transmitted packets from all transducers. With the estimated MIMO channel, one data block following the training blocks is equalized. The phase rotation in the equalized data block is compensated by a group-wise phase correction operation, before symbol detection. The newly detected data block along with $K-1$ previous data (or pilot) blocks are utilized to re-estimate the channel, which is employed to equalize the next new data block. The block-wise processing procedure is repeated until all blocks in the received packet are processed and demodulated. The proposed receiver scheme is tested with MakaiEx05 experimental data measured at Kauai, Hawaii, in September 2005. Processing results show that it works effectively with 2×8 BPSK, QPSK and 8PSK transmissions at the symbol period of 0.1 milliseconds. The average uncoded bit error rate (BER) is on the order of 8×10^{-4} for BPSK, 3×10^{-2} for QPSK, and 8×10^{-2} for 8PSK transmission.**

I. INTRODUCTION

High data rate underwater acoustic communications is known as a challenging task due to the extended multipaths delay spread and large Doppler spread of the underwater acoustic channels. Much progress has been made in this area in the last 15 years, see [1]-[9] and the references therein. Recently, motivated by the advancement of information theory and multiple-input multiple-output (MIMO) RF wireless systems [10]-[11], researchers have started to employ the RF MIMO technology for underwater acoustic channels to further increase the communication data rate [12]-[18].

In [12], [13], time-domain receiver design for MIMO underwater acoustic communications was investigated. In this scheme, which is a good extension of the seminal paper [2] in underwater acoustic phase-coherent communications, the canonical MIMO decision feedback equalizer (DFE) is jointly optimized with a second-order phase-locked loop (PLL) to perform equalization and phase synchronization. This scheme was successfully tested by underwater experiment with multi-band (six bands) transmission at data symbol period of 0.5 milliseconds (ms) for each band.

In [17], [18], frequency-domain MIMO receiver designs have been proposed for orthogonal frequency division multiplexing (OFDM) and single-carrier systems with successful underwater experimental results.

In this paper, we are going to extend the time-domain receiver structure of [19], [20], which was proposed for single-carrier single input multiple output (SIMO) underwater acoustic communications, to MIMO underwater acoustic communications. The receiver structure will decouple the equalization and phase correction into two separate block operations. The proposed receiver scheme is tested with experimental data measured off the northwestern coast of Kauai, Hawaii, in September 2005. The uncoded bit error rate (BER) results show that it works effectively with two-transmit data streams at symbol period of 0.1 ms with BPSK, QPSK and 8PSK modulations.

II. SYSTEM MODEL

For an underwater acoustic communication system employing N transducer sources and M hydrophone receivers, the discrete-time baseband equivalent signal received at the m-th receiver is expressed by

$$y_m(k) = \sum_{n=1}^{N} \sum_{l=0}^{L-1} h_{n,m}(k,l) x_n(k-l) e^{j[2\pi f_{n,m}(k)kT_s + \theta_{n,m}(0)]} + v_m(k) \tag{1}$$

where T_s is the symbol interval, $x_n(k)$ is the transmitted symbol from the n-th transducer at time instant k, $h_{n,m}(k,l)$, $f_{n,m}(k)$ and $\theta_{n,m}(0)$ are the l-th fading channel coefficient, the instantaneous Doppler and coarse synchronization phase error, respectively, between the n-th transducer and the m-th receiver at time k, $v_m(k)$ is zero-mean additive white Gaussian noise (AWGN) on the m-th receiver with power σ^2. In many practical underwater acoustic systems [1], [2], [6], [12], [13], the fading channel coefficient $h_{n,m}(k,l)$ usually changes much slower than the instantaneous phase $2\pi f_{n,m}(k)kT_s$, so it is proper to treat them separately. Denoting $\phi_{n,m}(k) \triangleq 2\pi f_{n,m}(k)kT_s + \theta_{n,m}(0)$, we are able to express (1) in more compact form

$$y_m(k) = \sum_{n=1}^{N} \sum_{l=0}^{L-1} h_{n,m}(k,l) x_n(k-l) e^{j\phi_{n,m}(k)} + v_m(k). \tag{2}$$

III. MIMO RECEIVER DESIGN

Fig. 1 depicts the block diagram of our time-domain MIMO receiver structure. In the following subsections, MIMO channel estimation and equalization will be discussed in detail.

		Form Approved OMB No. 0704-0188

Report Documentation Page

1. REPORT DATE **SEP 2008**	2. REPORT TYPE	3. DATES COVERED **00-00-2008 to 00-00-2008**

4. TITLE AND SUBTITLE	5a. CONTRACT NUMBER
Time-Domain Receiver Design for MIMO Underwater Acoustic Communications	5b. GRANT NUMBER
	5c. PROGRAM ELEMENT NUMBER
6. AUTHOR(S)	5d. PROJECT NUMBER
	5e. TASK NUMBER
	5f. WORK UNIT NUMBER

7. PERFORMING ORGANIZATION NAME(S) AND ADDRESS(ES) **Naval Research Laboratory,Washington,DC,20375**	8. PERFORMING ORGANIZATION REPORT NUMBER

9. SPONSORING/MONITORING AGENCY NAME(S) AND ADDRESS(ES)	10. SPONSOR/MONITOR'S ACRONYM(S)
	11. SPONSOR/MONITOR'S REPORT NUMBER(S)

12. DISTRIBUTION/AVAILABILITY STATEMENT **Approved for public release; distribution unlimited**

13. SUPPLEMENTARY NOTES **See also ADM002176. Presented at the MTS/IEEE Oceans 2008 Conference and Exhibition held in Quebec City, Canada on 15-18 September 2008. U.S. Government or Federal Rights License.**

14. ABSTRACT **see report**

15. SUBJECT TERMS

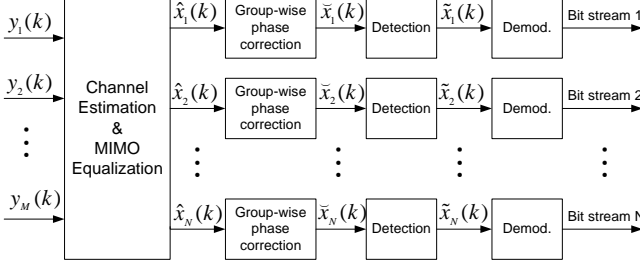| 16. SECURITY CLASSIFICATION OF:			17. LIMITATION OF ABSTRACT	18. NUMBER OF PAGES	19a. NAME OF RESPONSIBLE PERSON
a. REPORT **unclassified**	b. ABSTRACT **unclassified**	c. THIS PAGE **unclassified**	**Same as Report (SAR)**	**6**	

Fig. 1. New time-domain MIMO receiver structure, where the equalization and phase correction are decoupled.

A. MIMO Channel Estimation

Channel estimation is performed with pilot symbols $\{p_n(k), 1 \le n \le N, 0 \le k \le N_p-1\}$ from all transducers. When the time duration of the blocks of pilot symbols is less than the channel coherence time, the fading channel coefficient $h_{n,m}(k,l)$ in (2) can be approximately treated as time-invariant, i.e., $h_{n,m}(k,l) \approx h_{n,m}(l)$, and the differences among the phase drift sequence $\{\phi_{n,m}(k)\}$ are insignificant. Then (2) can be represented in matrix form as follows

$$\mathbf{y}_m = \mathbf{P}\mathbf{h}_m + \mathbf{v}_m \tag{3}$$

where

$$\mathbf{y}_m = [y_m(L-1), y_m(L), \cdots, y_m(N_p-1)]^T \tag{4}$$

$$\mathbf{P} = \begin{bmatrix} \mathbf{P}_1 & \mathbf{P}_2 & \cdots & \mathbf{P}_N \end{bmatrix} \tag{5}$$

$$\mathbf{P}_n = \begin{bmatrix} p_n(L-1) & \cdots & p_n(1) & p_n(0) \\ p_n(L) & \cdots & p_n(2) & p_n(1) \\ \vdots & \ddots & \ddots & \vdots \\ p_n(N_p-1) & \cdots & p_n(N_p-L+1) & p_n(N_p-L) \end{bmatrix} \tag{6}$$

$$\mathbf{h}_m = \begin{bmatrix} e^{j\phi_{1,m}(I)}\mathbf{h}_{1,m}^T & e^{j\phi_{2,m}(I)}\mathbf{h}_{2,m}^T & \cdots & e^{j\phi_{N,m}(I)}\mathbf{h}_{N,m}^T \end{bmatrix}^T \tag{7}$$

$$\mathbf{h}_{n,m} = [h_{n,m}(0), h_{n,m}(1), \cdots, h_{n,m}(L-1)]^T \tag{8}$$

$$\mathbf{v}_m = [v_m(L-1), v_m(L), \cdots, v_m(N_p-1)]^T \tag{9}$$

$(\cdot)^T$ represents vector transpose operation, and the index I in (7) is determined as $I = \lceil (N_p+L-2)/2 \rceil$ with $\lceil x \rceil$ denoting the smallest integer larger than x.

With (3), the least square (LS) and linear minimum mean square error (LMMSE) channel estimations are obtained as

$$\hat{\mathbf{h}}_m = \mathbf{P}^\dagger \mathbf{y}_m \tag{10}$$

and

$$\tilde{\mathbf{h}}_m = \left(\mathbf{P}^H\mathbf{P} + \sigma^2\mathbf{I}\right)^{-1}\mathbf{P}^H\mathbf{y}_m \tag{11}$$

where $\dagger$ denotes pseudo inverse of a matrix, $(\cdot)^H$ denotes vector or matrix Hermitian transpose, and $\mathbf{I}$ is $NL \times NL$ identity matrix. The estimations in (10) and (11) are performed on all M receivers to obtain MIMO channel estimation.

B. MIMO Equalization and Phase Compensation

With estimated channels, MIMO equalizer can then be designed. For a MIMO linear equalizer (LE), the equalized symbols of the n-th transmitted stream at time k, is given by

$$\hat{x}_n(k) = \sum_{m=1}^{M} \sum_{q=-K_1}^{K_2} c_{n,m}^{(q)} y_m(k-q) \tag{12}$$

where K_1, K_2 are nonnegative integers, $c_{n,m}^{(q)}$ denotes the q-th equalizer coefficient of the m-th receiver, for equalizing transmitted symbols from the n-th transducer.

Representing (12) in matrix form, and arranging the equalized symbols of all N transducers in vector, leads to

$$\hat{\mathbf{X}} = \mathbf{C}\mathbf{Y} \tag{13}$$

where $\mathbf{C} = \left[\mathbf{C}_1^T, \mathbf{C}_2^T, \cdots, \mathbf{C}_N^T\right]^T$, $\hat{\mathbf{X}} = [\hat{x}_1(k), \hat{x}_2(k), \cdots, \hat{x}_N(k)]^T$
$\mathbf{Y} = [y_1(k+K_1), \cdots, y_1(k-K_2), \cdots, y_M(k+K_1), \cdots, y_M(k-K_2)]^T$
$\mathbf{C}_n = \left[c_{n,1}^{(-K_1)}, c_{n,1}^{(-K_1+1)}, \cdots, c_{n,1}^{(K_2)}, \cdots, c_{n,M}^{(-K_1)}, c_{n,M}^{(-K_1+1)}, \cdots, c_{n,M}^{(K_2)}\right]$.

Using the MMSE criterion, we obtain the optimum MIMO LE coefficient matrix given by

$$\mathbf{C}_{\text{opt}} = E\left[\mathbf{X}\mathbf{Y}^H\right]\left\{E\left[\mathbf{Y}\mathbf{Y}^H\right]\right\}^{-1} \tag{14}$$

With the optimum equalizer taps, equalization can then be performed. Substituting (2) into (12), we get the n-th element of $\hat{\mathbf{X}}$ expressed as

$$\hat{x}_n(k) = \sum_{m=1}^{M}\left[\sum_{q=-K_1}^{K_2}\sum_{i=1}^{N}\sum_{l=0}^{L-1} c_{n,m}^{(q)} h_{i,m}(k-q,l)x_i(k-q-l)e^{j\phi_{i,m}(k-q)}\right] + \eta_n(k) \tag{15}$$

where $\eta_n(k) = \sum_{m=1}^{M}\sum_{q=-K_1}^{K_2} c_{n,m}^{(q)} v_m(k-q)$ is the collection of additive noise $v_m(k)$ on all M receivers at the n-th output of MIMO equalizer. As we can see from (15), the triple summation in the square bracket is the equalizer's contribution of the m-th receiver to the n-th transducer. Therefore, we can define

$$\alpha_{n,m}(k)x_n(k) \triangleq \sum_{q=-K_1}^{K_2}\sum_{i=1}^{N}\sum_{l=0}^{L-1} c_{n,m}^{(q)} h_{i,m}(k-q,l)x_i(k-q-l)e^{j\phi_{i,m}(k-q)}$$

where $\alpha_{n,m}(k)$ denotes the scaling factor corresponding to the mth receiver, and it is usually a complex value closely related to equalizer taps $c_{n,m}^{(q)}$ and instantaneous phase rotation $e^{j\phi_{i,m}(k-q)}$. With above definition, (15) is simplified as

$$\hat{x}_n(k) = |\gamma_n(k)| e^{j\angle\gamma_n(k)}x_n(k) + \eta_n(k) \tag{16}$$

where $\gamma_n(k) = \sum_{m=1}^{M}\alpha_{n,m}(k)$ is actually the diversity combining gain of M receivers.

Obviously, the M-receiver equalized symbol of the n-th transducer in (16) is an amplitude-scaled and phase-rotated version of the originally transmitted symbol. The phase rotation $\angle\gamma_n(k)$, which is ultimately caused by instantaneous Doppler spread $f_{n,m}(k)$ and initial timing-error phase offset $\theta_{n,m}(0)$, must be compensated for systems employing coherent modulation scheme for achieving good detection

performance. We adopt a MIMO group-wise phase estimation and correction method to compensate the phase rotations in the equalized symbols, and the details are referred to [22], which is an extension from the SIMO case [19].

C. Layered space-time receiver design

Layered space-time receiver structure was first proposed by Foschini [23], namely D-BLAST, for frequency flat fading channels. This technique was extended in [24] for frequency-selective channels, where the layered equalization scheme based on the ordered successive interference cancelation (OSIC) is proposed, and proved to be superior to conventional equalization. In the OSIC scheme, transmitted streams are detected in an order that strong streams are equalized and detected earlier, and each stream is equalized with the co-channel interference (CCI) from all previously detected streams already subtracted out.

The key for the success of the OSIC-based layered equalization is the consequent reconstruction and cancelation of CCI. When the n-th transmitted stream is detected, the corresponding CCI is reconstructed on the m-th receiver as

$$\hat{I}_{n,m}(k) = \sum_{l=0}^{L-1} h_{n,m}(k,l)\bar{x}_n(k) \tag{17}$$

where

$$\bar{x}_n(k) = \tilde{x}_n(k)e^{j(\angle\hat{x}_n(k)-\angle\tilde{x}_n(k))} \tag{18}$$

with $\hat{x}_n(k)$ and $\tilde{x}_n(k)$ being the equalized symbol and the detected symbol of the n-th transmitter, respectively, as shown in Fig. 1. The reconstructed interference is then subtracted from $y_m(k)$ as

$$\tilde{y}_m(k) = y_m(k) - \hat{I}_{n,m}(k) \tag{19}$$

and the updated received samples are used for equalizing the next stream in the order until all streams are equalized and detected.

IV. EXPERIMENTAL RESULTS

Single-band and multi-band underwater MIMO experiments were conducted off the northwestern coast of Kauai, Hawaii, in September 2005. The multi-band transmission has six bands in total and each band has data symbol period of 0.5 ms. The multi-band experimental data were processed by the algorithms presented in [13] with successful results for various number of transducer sources.

In this paper, we are focusing on the single-band transmission experimental data with data symbol period of 0.1 ms with two transducer sources. For this single-band experiment, the centered carrier frequency is $f_c = 32$ kHz, data bandwidth is $f_b = 10$ kHz plus 4 kHz due to the square-root raised cosine pulse shaping filter with roll-off factor being 0.4. BPSK, QPSK and 8PSK are employed for the data modulations. Ten transducers are available for transmitting signals, and eight hydrophones are used to receive signals.

The modulated data symbols are transmitted in packets, and the structure of one packet is shown in Fig. 2. Each packet consists of three parts: the first part is a sequence of 10 consecutive probe signals, each having a duration of 0.4 seconds, transmitted by transducers 1 to 10 sequentially, plus a 0.2 seconds clear time at the end. The second part is the data payload with a time duration of 4.8 seconds. Different from probe signals which are always transmitted sequentially by all 10 transducers, data signals are transmitted simultaneously only from selected transducers. The number of selected transducers N varies from 1 to 10, so that MIMO communications with different number of transmitters can be implemented. The last part is a 3-seconds clear time used for transmission system re-synchronization. The whole transmitted packet has a time duration of 12 seconds.
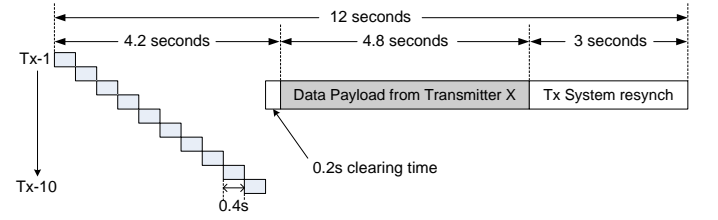

Fig. 2. Packet structure.

Each of the ten probe signals contains a linear frequency modulation (LFM) signal, which is used for packet coarse synchronization in light of its good correlation characteristic. Moreover, the channel length L is also estimated with LFM signal by measuring the span of the LFM correlation main ridge [20]. It's shown that for all MIMO subchannels, most of the channel energy is concentrated within 10 ms which corresponds to a channel length of $L = 100$ in terms of symbol interval $T_s = 0.1$ ms.

The 4.8-seconds received data package contains 48000 symbols at the symbol period of 0.1 ms. It's artificially partitioned into blocks for processing. We chose the block size $N_b = 200$ symbols, which corresponds to a 0.02 seconds time duration. As described in Section III-A, the MIMO channel is initially estimated using training blocks located at the front of data packages from all N transducers. For the channel length of $L = 100$, $4 \sim 6$ training blocks, which corresponding to a training length N_p of $800 \sim 1200$ symbols, are flexibly selected depending on the requirement for estimation accuracy. Figs. 3 and 4 show samples of the estimated channel impulse responses (CIRs) for the two-transmitter eight-receiver BPSK and QPSK transmissions, respectively. Obviously, over the depicted delay spread of 15 ms, each of the subchannels contains two CIR peaks located at 2 ms and 6 ms, respectively, and we chose 10 ms as the delay spread for channel estimation. The estimated MIMO CIRs with 8PSK transmission are similar to those depicted in Fig. 4, details are omitted for brevity.

The estimated MIMO channel is employed to equalize a block of N_b symbols following the pilot symbols. The N_b equalized symbols are then fed into the group-wise phase correction unit for phase estimation and compensation, as shown in Fig. 1. A group size of $N_s = 20$ is used, and there are $N_g = 10$ groups in one block. After phase-correction, the N_b symbols are detected. To effectively track the variation
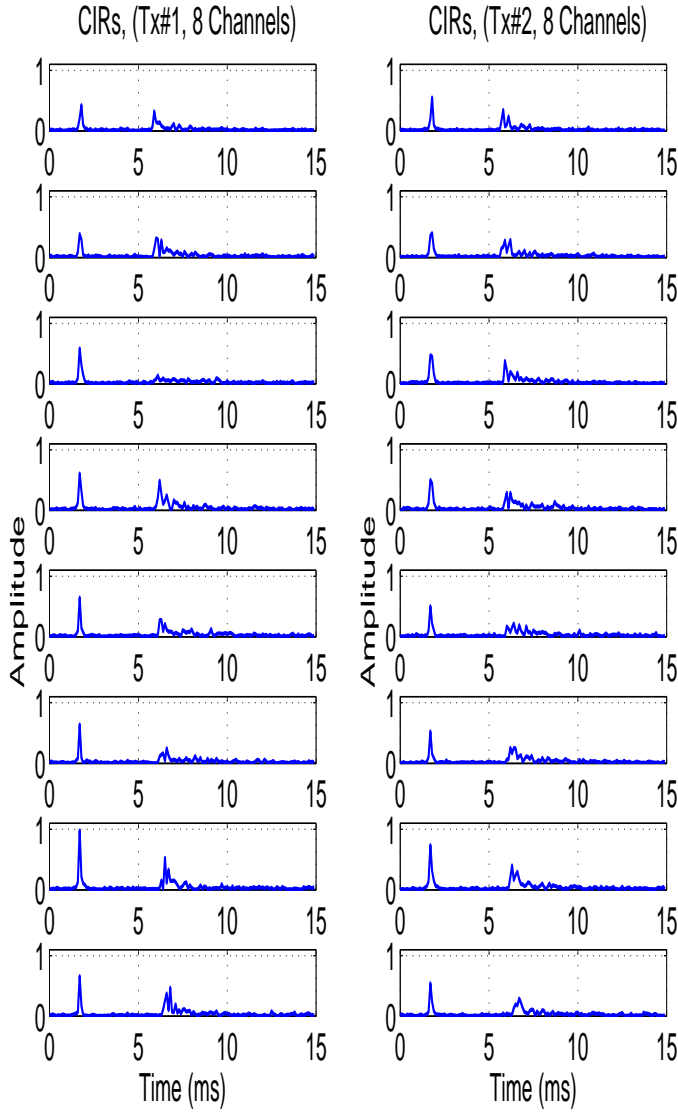
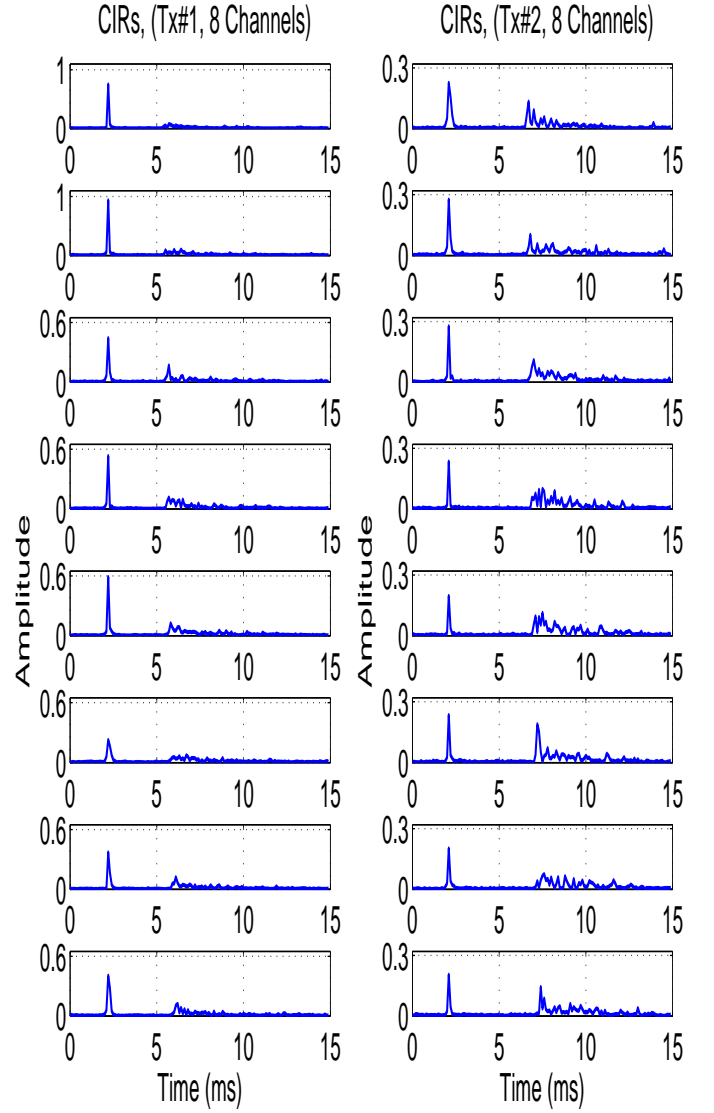Fig. 3. Estimated channel impulse responses for two-transmitter eight-receiver system with BPSK transmission.

Fig. 4. Estimated channel impulse responses for two-transmitter eight-receiver system with QPSK transmission.

of channel, the N_b newly detected symbols are combined with $K - 1$ previous blocks of detected symbols (or pilots) to re-estimate the MIMO channel, as shown in Fig 5. The parameter K is selected so that the time duration of K blocks doesn't exceed the channel coherence time. In the processing of practical packets, K equaling to 4, 5 or 6 are selected. With the updated channel, N_b new symbols are equalized and detected in a similar way mentioned above. The channel re-estimation and detection procedure continues until the whole data packet is processed. To combat possible error propagation, we estimate the channel using training symbols every Q blocks, where Q is properly selected so that the overhead of training symbols can be minimized. We choose $Q = 80$ in the processing. It is noteworthy that, for a partition block size of 200, each packet contains 240 blocks in total. Therefore, the choice of $Q = 80$ incurs three times of channel estimation

based on training blocks in the processing of a whole packet, which is 5%-7.5% overall training overhead with each training set containing $4 \sim 6$ blocks. It is also noted that conventional algorithms usually have 20% training overhead [13], [25].
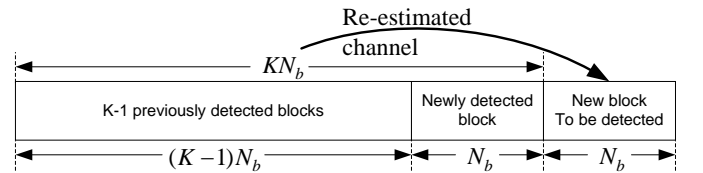

Fig. 5. Channel re-estimation.

The scatter plots in Figs. 6 and 7 are the original received baseband signals, and the equalized and phase-corrected BPSK signals, respectively, with a 2×8 MIMO implementation.

Fig. 7 clearly indicates that most of the symbols can be properly classified. The equalized and phase-corrected QPSK and 8PSK symbols are depicted in Fig. 8 and Fig. 9, respectively. Similar observations are found as that for BPSK modulation.
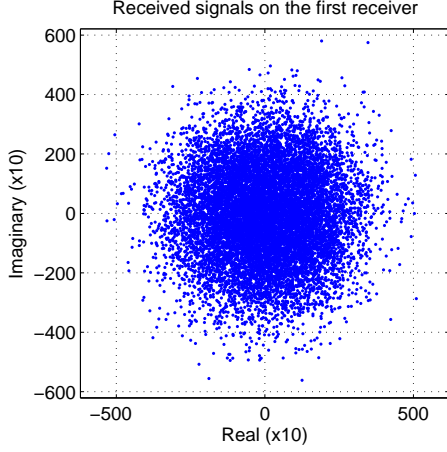

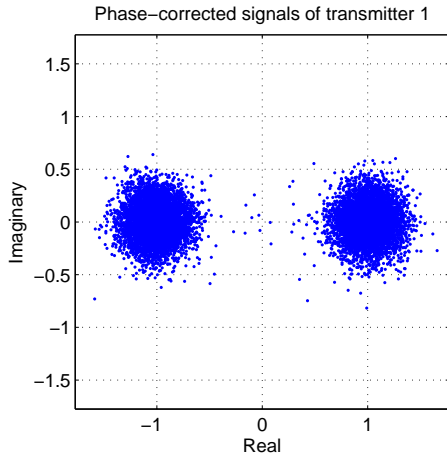Fig. 6.   Scatter plot of received BPSK signals at the first receiver.

Fig. 7.   Phase-corrected BPSK signals with eight-receiver combining.

From the available experimental data, we have eight packets of 2×8 BPSK data, three packets of 2×8 QPSK data, and two packets of 2×8 8PSK data. We processed all these packets by our proposed receiver structure. The uncoded bit error rate (BER) results with eight-receiver combining for the 2×8 BPSK, QPSK and 8PSK packets are listed in Tables 1–3. From these tables, we make the following observations. First, it is clear that BPSK transmission has the best average uncoded BER on the order of 8×10^{-4}, and QPSK has better uncoded BER than 8PSK. This observation is as expected since under the same transmission conditions, using larger constellation size always degrades uncoded BER performance. The second observation comes from the BER comparison between the two transmitters. For BPSK transmission, the average uncoded BERs for the two transmitters are comparable, as can be seen
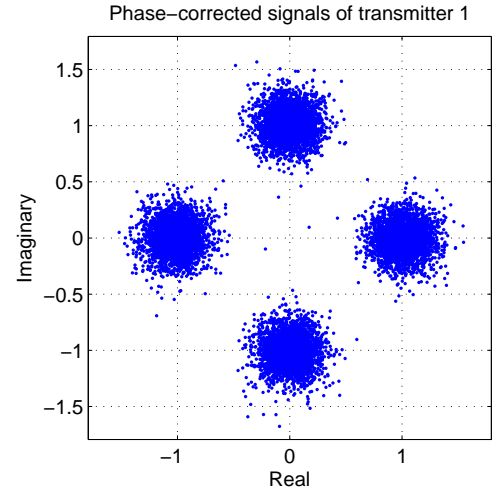

Fig. 8.   Phase-corrected QPSK signals with eight-receiver combining.
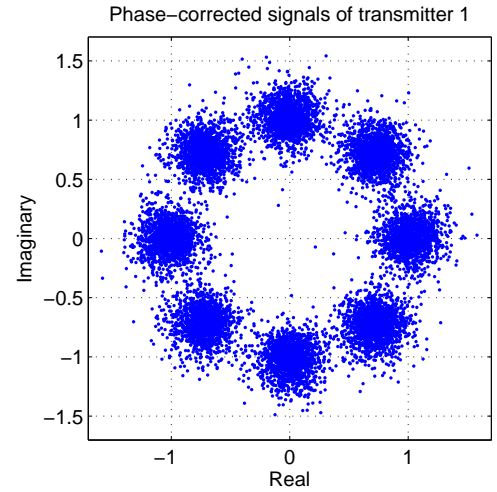

Fig. 9.   Phase-corrected 8PSK signals with eight-receiver combining.

in the last line of Table 1. However, for QPSK and 8PSK transmission, Transmitter 1 has better BER than Transmitter 2. This is because that the channel impulse responses associated with Transmitter 1 contain larger average power than those associated with Transmitter 2, which is indicated in Fig. 4.

Table 1: Uncoded BER of 2×8 BPSK transmission

Packet index	BER of Tx 1	BER of Tx 2	BER of Tx 1&2
1	2.800e-3	4.178e-3	3.489e-3
2	4.237e-4	1.695e-4	2.966e-4
3	1.556e-3	9.333e-4	1.244e-3
4	1.316e-4	5.482e-4	3.399e-4
5	2.412e-4	1.096e-4	1.695e-4
6	4.240e-5	1.271e-4	8.475e-5
7	8.114e-4	5.044e-4	6.579e-4
8	1.059e-4	6.360e-5	8.475e-5
Mean	7.645e-4	8.294e-4	7.954e-4

Table 2: Uncoded BER of 2×8 QPSK transmission

Packet index	BER of Tx 1	BER of Tx 2	BER of Tx 1&2
1	1.656e-3	1.756e-1	8.863e-2
2	1.126e-4	1.707e-2	8.592e-3
3	1.351e-4	1.498e-3	8.164e-4
Mean	6.346e-4	6.472e-2	3.268e-2

Table 3: Uncoded BER of 2×8 8PSK transmission

Packet index	BER of Tx 1	BER of Tx 2	BER of Tx 1&2
1	8.213e-3	1.614e-1	8.481e-2
2	1.669e-2	1.199e-1	6.831e-2
Mean	1.245e-2	1.407e-1	7.656e-2

V. CONCLUSION

We have demonstrated a time-domain MIMO receiver structure, which separates equalization and phase correction operations, for high data rate single-carrier underwater acoustic communications. MIMO channel estimation is initially obtained with training symbols, and then updated with newly detected symbols, so that the channel estimation can be implemented while the training overhead is as low as $5\% \sim 7.5\%$. The low-complexity MIMO linear equalizer is operated with ordered successive interference cancelation to perform layered space-time equalization. The proposed structure is tested with experimental data measured off the northwestern coast of Kauai, Hawaii, in September 2005. Processing results show that it works effectively with 2×8 BPSK, QPSK and 8PSK transmission at the symbol period of 0.1 ms. The gross data rate is 20, 40 and 60 kilo-bits per second for BPSK, QPSK and 8PSK, respectively. The average uncoded BER is on the order of 8×10^{-4} for BPSK, 3×10^{-2} for QPSK, and 8×10^{-2} for 8PSK transmission.

REFERENCES

[1] M. Stojanovic, J. Catipovic, and J. Proakis, "Adaptive multichannel combining and equalziation for underwater acoustic communications," *J. Acoust. Soc. Amer.*, vol.94, pp.1621-1632, Jan. 1993.

[2] M. Stojanovic, J. Catipovic, and J. Proakis, "Phase-coherent digital communicaitons for underwater acoustic channels," *IEEE J. Ocean Eng.*, vol.19, pp.100-111, Jan. 1994.

[3] D. B. Kilfoyle and A. B. Baggeroer, "The state of the art in underwater acoustic telemetry," *IEEE J. Ocean. Eng.*, vol.25, pp.4-27, Jan. 2000.

[4] B. S. Sharif, J. Neasham, O. R. Hinton, and A. E. Adams, "A computationally efficient Doppler compensation system for underwater acoustic communications," *IEEE J. Ocean Eng.*, vol.25, pp.52-61, Jan. 2000.

[5] T. H. Eggen, A. B. Baggeroer, and J. C. Preisig, "Communication over Doppler spread channels – Part I: channel and receiver presentation," *IEEE J. Ocean Eng.*, vol.25, pp.62-71, Jan. 2000.

[6] T. C. Yang, "Differences between passive-phase conjugation and decision-feedback equalizer for underwater acoustic communications," *IEEE J. Ocean Eng.*, vol.29, pp.472-487, April 2004.

[7] T. C. Yang, "Correlation-based decision-feedback equalizer for underwater acoustic communications," *IEEE J. Ocean Eng.*, vol.30, pp.865-880, Oct. 2005.

[8] J. C. Preisig, "Performance analysis of adaptive equalization for coherent acoustic communications in the time-varying ocean environment," *J. Acoust. Soc. Am.*, vol.118, pp.263-278, 2005.

[9] B. Li, S. Zhou, M. Stojanovic, L. Freitag, and P. Willett, "Non-uniform doppler compensation for zero-padded OFDM over fast-varying underwater acoustic channels," *Proc. OCEANS'07*, 18-21 June 2007.

[10] G. J. Foschini and M. J. Gans, "On limits of wireless communications in a fading environment when using multiple antennas," *Wireless Personal Communications*, vol. 6, pp. 311-335, March 1998.

[11] I. E. Telatar, "Capacity of a mulit-antenna Gaussian channels," *European Trans. on Telecommunications*, vol. 10, pp. 585-595, Nov. 1999.

[12] S. Roy, T. M. Duman, V. McDonald, and J. Proakis, "Enhanced underwater acoustic communication performance using space-time coding and processing," in *Proc. Ocean'04*, 2004.

[13] S. Roy, T. M. Duman, V. McDonald, and J. Proakis, "High rate communication for underwater acoustic channels using multiple transmitters and space-time coding: receiver structures and experimental results," *IEEE J. Ocean. Eng.*, vol.32, pp.663-688, July 2007.

[14] D. B. Kilfoyle, J. C. Preisig, and A. B. Baggeroer, "Spatial modulation expreiments in underwter acoustic channel," *IEEE J. Ocean. Eng.*, vol.30, pp.406-415, April 2005.

[15] H. C. Song, P. Roux, W. S. Hodgkiss, W. A. Kuperman, T. Akai, and M. Stevenson, "Multiple-input-multiple-output coherent time reversal communications in a shallow-water acoustic channel," *IEEE J. Ocean. Eng.*, vol.31, pp.170-187, Jan. 2006.

[16] R. F. Ormondroyd, "A robust underwater acoustic communication system using OFDM-MIMO," in *Proc. Oceans'07*, June 2007

[17] B. Li, S. Zhou, M. Stojanovic, L. Freitag, J. Huang, and P. Willett, "MIMO-OFDM over an underwater acoustic channel," in *Proc. Oceans'07*, Sept. 2007.

[18] J. Zhang, Y. R. Zheng, and C. Xiao, "Frequency-domain equalization for single-carrier MIMO underwater acoustic communications," in *Proc. OCEANS'08*, Sept. 2008.

[19] Y. R. Zheng, "Channel estimation and phase-correction for robust underwater acoustic communications," in *Proc. IEEE Military Communications Conf. (MilCom07)*, Orlando, Oct. 2007.

[20] J. Tao, Y. R. Zheng, C. Xiao, T. C. Yang, and W. B. Yang "Channel estimation, equalization and phase correction for single carrier underwater acoustic communications," in *Proc. Oceans'08*, Kobe, Japan, April 2008.

[21] J.G. Proakis and M. Salehi, *Digital Communication*, 5th Ed. Upper Saddle River, NJ: McGraw-Hill, 2008.

[22] C. Xiao and Y. R. Zheng, "Channel equalization and symbol detection for single carrier broadband MIMO systems with multiple carrier frequency offsets" in *Proc. 2008 IEEE ICC*, pp.4316-4320, Beijing, China, 19-23 May 2008.

[23] G. J. Foschini, "Layered space-time architecture for wireless communication in a fading environment when using multiple antennas," *Bell Labs Technical Journal*, vol. 1, no. 2, pp. 41-59, Autumn 1996.

[24] A. Lozano and C. Papadias, "Layered space-time receivers for frequency-selective wireless channels," *IEEE Trans. on Commun.*, vol.50, pp.65-73, Jan. 2002.

[25] M. V. Clark, "Adaptive frequency-domain equalization and diversity combining for broadband wireless communications," *IEEE J. Select Areas Commun.*, vol.16, pp.1385-1395, Oct. 1998.